

# A non-homogeneous ground state of the low-temperature Sakai-Sugimoto model

---

**C.A. Ballon Bayona, Kasper Peeters and Marija Zamaklar**

*Department of Mathematical Sciences,  
Durham University,  
South Road,  
Durham DH1 3LE,  
United Kingdom.*

*E-mail:* [c.a.m.ballonbayona@durham.ac.uk](mailto:c.a.m.ballonbayona@durham.ac.uk),  
[kasper.peeters@durham.ac.uk](mailto:kasper.peeters@durham.ac.uk), [marija.zamaklar@durham.ac.uk](mailto:marija.zamaklar@durham.ac.uk)

**ABSTRACT:** We study the instability of the low-temperature QCD vacuum at large- $N_c$  due to an axial chemical potential, using the holographic Sakai-Sugimoto model. We explicitly construct the ground state of the theory, which corresponds to a translationally non-invariant configuration.

**KEYWORDS:** AdS/QCD, chemical potential, chiral density wave

---

## Contents

<b>1</b>	<b>Introduction</b>	<b>1</b>
<b>2</b>	<b>Chemical potentials in the Sakai-Sugimoto model</b>	<b>3</b>
2.1	Review of the model	3
2.2	Holographic realisation of chemical potentials	6
<b>3</b>	<b>The spatially modulated phase</b>	<b>8</b>
3.1	Equations of motion	8
3.2	The abelian ansatz	9
3.3	Analysis of the ground state	11
<b>4</b>	<b>Spatially modulated phase for the DBI action</b>	<b>16</b>
4.1	Stability analysis	17
4.2	Ground state: Maxwell versus DBI	19
<b>5</b>	<b>Discussion and open questions</b>	<b>19</b>
<b>6</b>	<b>Appendix: The Hamiltonian</b>	<b>21</b>
6.1	Maxwell truncation	21
6.2	DBI-CS Hamiltonian	22

---

## 1 Introduction

The behaviour of QCD at non-zero temperature and density is an active area of research both from a theoretical as well as an experimental perspective. While perturbation theory can be used at very large temperatures or densities, this is of limited use in intermediate regimes such as those that are relevant for heavy ion collisions or the description of the interior of neutron stars, where QCD is strongly coupled. Lattice methods in turn are hard to apply to highly time-dependent processes, and also pose difficulties when dealing with systems with large baryon density because of the sign problem. Alternative techniques are therefore called for. The gauge/gravity duality provides a non-conventional approach to the study of strongly coupled gauge theories, and while the dual of QCD proper is not known (not even in the large- $N_c$  limit), some of the current proposals for holographic duals of gauge theories do at least seem to capture several qualitative properties of strongly coupled QCD.

One of the key questions related to QCD at non-zero quark chemical potential is that of the character of the ground state. Various models suggest that, for particular

values of the chemical potential and temperature, an instability sets in which results in the decay of the homogeneous vacuum to one which breaks translational invariance (see for instance the ladder analysis of QCD in the large- $N_c$  limit by Deryagin, Grigoriev and Rubakov [1]). In the dual holographic language, chemical potentials are typically realised by introducing an electric gauge field configuration on the world-volume of a flavour brane, with the non-normalisable component being related to the value of the chemical potential. Such electric configurations in the presence of a curved background can become unstable, as was emphasised in work of Nakamura, Park and Ooguri [2]. These authors have pointed out that a black hole with a constant electric field in five-dimensional Maxwell-Chern-Simons theory is unstable against decay towards a configuration with both electric and magnetic fields turned on. Importantly, this instability occurs only for a non-vanishing value of the spatial momentum  $k$ , signalling that the new ground state is spatially modulated. The lowest energy state has a uniquely specified momentum  $k_{\text{gs}}$ , which is determined by the value of the electric field. The origin of the instability can be traced to the presence of a Chern-Simons coupling.

In the context of holographic models, such behaviour was in fact first found in the work of Harvey and Domokos [3], who exhibited an instability in a particular bottom-up model with a Chern-Simons coupling and an axial chemical potential. More recently, Ooguri and Park [4, 5] have analysed the Sakai-Sugimoto model [6, 7] in the *deconfined* phase, where chiral symmetry is restored. This model contains Chern-Simons couplings in the action of flavour D8-branes. The presence of a non-vanishing electric field corresponding to a quark chemical potential then leads to an instability towards a phase where baryonic charge density is generated. This non-homogeneous ground state contains corresponding baryonic and axial currents carrying non-zero momenta  $k_{\text{gs}}$ .

This still leaves open the question as to whether a similar instability can occur at vanishing temperature. In the aforementioned Sakai-Sugimoto model, it is known that even at zero temperature, a sufficiently large *isospin* chemical potential can lead to an instability towards a new ground state in which vector mesons condense [8]. This ground state, even though it breaks rotational invariance, is spatially homogeneous. The question remains whether a non-homogeneous ground state is possible in this model. In the present paper, we therefore set out to use the holographic model of Sakai and Sugimoto to study the properties of a QCD-like theory in the large- $N_c$  limit, at non-vanishing values of the *axial* chemical potential.<sup>1</sup> More precisely, we

---

<sup>1</sup>An axial chemical potential is induced by a time-dependent theta angle, and as such is one of the motivations to study the Chiral Magnetic Effect [9], where theta angle fluctuations together with a magnetic field induce an electric current. The axial potential also plays an important role in the holographic realisation of chiral magnetic spirals [10]. In the present paper, however, we do not turn on any additional magnetic field but simply study the consequence of the axial chemical

analyse the ground state in the *confining* phase where *chiral symmetry is broken*. Although the axial currents are anomalous in real QCD, this anomaly is suppressed in the large- $N_c$  limit, and the axial  $U(1)$  current is conserved. We will see that this potential can trigger an instability to a new non-homogeneous ground state. This is to be contrasted with the effect of a baryon chemical potential. The latter would lead to condensation of baryons, which are somewhat problematic in the large- $N_c$  limit as they become infinitely heavy, and are in fact singular objects in the Sakai-Sugimoto model.<sup>2</sup> Our solutions are regular and have finite energy.<sup>3</sup>

Our results show that even the low-temperature phase of the Sakai-Sugimoto is unstable against decay into a non-homogeneous state. These results can be contrasted with recent work [12] on the effects of the axial chemical potential in the PLSM $_q$  model, where no evidence for an axial potential induced phase transition at zero temperature was found. The spatial modulation of the ground state we find is characterised by the momentum, which is interestingly, to good approximation independent of the axial density (or chemical potential). We also find that the axial density of the new ground state is substantially larger for a given chemical potential than in the homogeneous phase. The instabilities towards new ground state occur both in the Maxwell-Chern-Simons truncation of the flavour D8-brane action as well as in the full DBI system, provided the Chern-Simons coupling of the latter is sufficiently large. We do not find any evidence for condensation into other states as the chemical potential is increased further. While new non-homogeneous configurations appear, they do not correspond to new global energy minima, but only to new meta-stable vacua, as they have larger free energy than the true ground state.

## 2 Chemical potentials in the Sakai-Sugimoto model

### 2.1 Review of the model

In this section we briefly review the basics of Sakai-Sugimoto model [6, 7] in order to set the scene and to introduce the conventions we will be using in this paper. The Sakai-Sugimoto model at low temperature is derived by considering the decoupling limit of a large number  $N_c$  of D4-branes compactified on a circle of radius  $R$  spanned by the coordinate  $\tau$ . Anti-periodic boundary conditions are imposed on the fermions. The system furthermore includes  $N_f$  flavour D8-branes positioned at  $\tau = 0$  and  $N_f$  anti-D8-branes positioned at  $\tau = L$ . The dual gauge theory is a maximally supersymmetric  $SU(N_c)$  gauge theory in 4+1 dimensions, which is compactified on a

---

potential by itself.

<sup>2</sup>The authors of [11] found a dynamical instability treating the baryonic chemical potential as a source of cusps in the flavour D8-branes.

<sup>3</sup>Because the solutions originate from the Chern-Simons term, they are of course still such that the fields scale as  $\sim \lambda$ , i.e. their scale is set by the string length.

circle with anti-periodic boundary conditions for the adjoint fermions, coupled to  $N_f$  left-handed fermions in the fundamental representation of  $SU(N_c)$  localised at  $\tau = 0$  and  $N_f$  right-handed fermions in the fundamental representation localised at  $\tau = L$ .

In more detail, the background generated by the stack of D4-branes has a metric, Ramond-Ramond four-form and string coupling given by

$$\begin{aligned} ds^2 &= \frac{U^{3/2}}{R^{3/2}} \eta_{\mu\nu} dx^\mu dx^\nu + \frac{U^{3/2}}{R^{3/2}} f(U) d\tau^2 + \frac{R^{3/2}}{U^{3/2}} \frac{dU^2}{f(U)} + R^{3/2} U^{1/2} d\Omega_4^2, \\ e^\phi &= g_s \frac{U^{3/4}}{R^{3/4}}, \quad F_4 = \frac{(2\pi l_s)^3 N_c}{V_{S^4}} \epsilon_4, \quad f(U) = 1 - \frac{U_{KK}^3}{U^3}, \end{aligned} \quad (2.1)$$

where  $\epsilon_4$  is the volume form on  $S^4$  and  $V_{S^4}$  its volume. The index  $\mu = 0, 1, 2, 3$  defines the directions of the dual gauge theory, and  $\tau$  is a coordinate on the circle so that  $\tau \equiv \tau + \delta\tau$ . The curvature radius is given by  $R = (\pi g_s N_c)^{1/3} l_s$  where  $g_s$  is the string coupling and  $l_s = \sqrt{\alpha'}$  is the string length. The period of the compact coordinate introduces a four-dimensional mass scale

$$\delta\tau = \frac{4\pi R^{3/2}}{3 U_{KK}^{1/2}} \equiv \frac{2\pi}{M_{KK}}, \quad (2.2)$$

and the four dimensional 't Hooft constant is related to the string coupling by

$$\lambda = g_{YM}^2 N_c = 2\pi M_{KK} g_s N_c l_s. \quad (2.3)$$

For our purposes it will also be convenient to introduce use pair of dimensionless coordinates  $y$  and  $z$  defined by the relations

$$U = U_{KK} (1 + y^2 + z^2)^{1/3} \equiv U_{KK} K_{y,z}^{1/3}, \quad \tau = \frac{\delta\tau}{2\pi} \arctan\left(\frac{z}{y}\right). \quad (2.4)$$

In terms of these coordinates the metric takes the form

$$\begin{aligned} ds^2 &= U_{KK}^{3/2} R^{-3/2} K_{y,z}^{1/2} \eta_{\mu\nu} dx^\mu dx^\nu + \frac{4}{9} R^{3/2} U_{KK}^{1/2} \frac{K_{y,z}^{-5/6}}{y^2 + z^2} \left[ (z^2 + y^2 K_{y,z}^{1/3}) dz^2 \right. \\ &\quad \left. + (y^2 + z^2 K_{y,z}^{1/3}) dy^2 + 2yz(1 - K_{y,z}^{1/3}) dy dz \right] + R^{3/2} U_{KK}^{1/2} K_{y,z}^{1/6} d\Omega_4^2. \end{aligned} \quad (2.5)$$

In this background one introduces a probe D8-brane and  $\overline{D8}$ -brane which fill out the 3 + 1 dimensional space-time and the four-sphere, and trace out a curve in the remaining two directions  $(U, \tau)$ . The latter coordinates span a two dimensional cigar-like subspace. The shape of the curve is obtained by solving the equation of motion of the probe branes, and is given by a one parameter family, which is specified by the asymptotic separation between the D8 and  $\overline{D8}$ -brane. In this paper we will be interested in the so-called antipodal brane embedding corresponding to the maximal, antipodal separation of the branes in the circular direction  $\tau$ . In this case, the branes

extend all the way to the tip of the cigar where they join in a smooth way. For this special case the metric on the brane world-volume takes the form

$$\begin{aligned} ds_{D8} &= U_{KK}^{3/2} R^{-3/2} K_z^{1/2} \eta_{\mu\nu} dx^\mu dx^\nu + \frac{4}{9} R^{3/2} U_{KK}^{1/2} K_z^{-5/6} dz^2 + R^{3/2} U_{KK}^{1/2} K_z^{1/6} d\Omega_4^2 \\ &\equiv G_{MN} dx^M dx^N, \end{aligned} \quad (2.6)$$

where  $K_z = 1 + z^2$ .

The action for the  $U(N_f)$  gauge fields living on the D8- $\overline{\text{D8}}$ -branes is given by the DBI action which in the non-abelian limit is not fully known, but at the quadratic order reduces just to the Yang-Mills action in a curved background, corresponding to the curved world-volume of the brane,

$$S_{\text{YM}} = -\mu_8 (\pi\alpha')^2 \int d^4x dz d^4\Omega e^{-\phi} \sqrt{-|G|} \text{Tr} (\mathcal{F}^{MN} \mathcal{F}_{MN}) \quad (2.7)$$

where  $\mathcal{F}_{MN} = \partial_M \mathcal{A}_N - \partial_N \mathcal{A}_M + i[\mathcal{A}_M, \mathcal{A}_N]$ , and the index  $m = (\mu, z, \alpha)$ . The coordinate  $z$  spans the holographic direction and  $\alpha$  labels the directions on  $S^4$ ; indices are raised or lowered using the metric (2.6). In order to avoid non-singlet  $SO(5)$  states associated to the  $S^4$ , in what follows we will set all the excitations along the sphere directions to zero,  $\mathcal{A}_\alpha = 0$  and assume that  $\mathcal{A}_\mu$  and  $\mathcal{A}_z$  do not depend on the  $S^4$  coordinates. Then we can integrate out the  $S^4$  coordinates and the Yang-Mills action reduces to

$$S_{\text{YM}} = -\kappa \int d^4x dz \text{Tr} \left[ \frac{1}{2} K_z^{-1/3} \eta^{\mu\rho} \eta^{\nu\sigma} \mathcal{F}_{\mu\nu} \mathcal{F}_{\rho\sigma} + M_{KK}^2 K_z \eta^{\mu\nu} \mathcal{F}_{\mu z} \mathcal{F}_{\nu z} \right] \quad (2.8)$$

where

$$\kappa = \frac{\sqrt{\alpha'} g_s N_c^2 M_{KK}}{108\pi^2} = \frac{\lambda N_c}{216\pi^3}. \quad (2.9)$$

Note that the Yang-Mills action can now be written in terms of an effective five-dimensional metric

$$ds_{(5)}^2 = g_{mn} dx^m dx^n = M_{KK}^2 K_z^{2/3} \eta_{\mu\nu} dx^\mu dx^\nu + K_z^{-2/3} dz^2, \quad (2.10)$$

in terms of which it takes the form

$$S_{\text{YM}} = -\frac{\kappa}{2} \int d^4x dz \sqrt{-g} \text{Tr} [\mathcal{F}^{mn} \mathcal{F}_{mn}], \quad (2.11)$$

where the indices are now raised or lowered using the metric  $g_{mn}$ .

The effective action for the D8 brane includes also a Chern-Simons term which is given by

$$S_{\text{CS}} = \mu_8 \frac{(2\pi\alpha')^3}{3!} \int_{D8} \omega_5 \wedge F_4 = \alpha \int \omega_5, \quad \alpha = \hat{\alpha} \frac{N_c}{24\pi^2}. \quad (2.12)$$

Here  $\hat{\alpha} = 1$  in string theory but we will keep it as a separate parameter for later use<sup>4</sup>. Again,  $F_4$  is the Ramond-Ramond four-form, proportional to the volume form of  $S^4$  (see (2.1)), and the  $\omega_5$  form is the usual five-dimensional Chern-Simons form,

$$\omega_5 = \text{Tr} \left( \mathcal{A} \mathcal{F}^2 - \frac{i}{2} \mathcal{A}^3 \mathcal{F} - \frac{1}{10} \mathcal{A}^5 \right). \quad (2.13)$$

It is useful for our purposes to decompose the  $U(N_f)$  gauge field into the  $SU(N_f)$  part  $\tilde{\mathcal{A}}$  and the  $U(1)$  part  $\hat{\mathcal{A}}$  as

$$\mathcal{A} = \tilde{\mathcal{A}} + \frac{1}{\sqrt{2N_f}} \hat{\mathcal{A}} \quad (2.14)$$

For the case  $N_f = 2$ , we can decompose the  $U(2)$  symmetry into the baryon  $U(1)$  and isospin  $SU(2)$ , and the Chern-Simons term decomposes as

$$S_{\text{CS}} = \alpha \int \left( \frac{3}{2} \hat{\mathcal{A}} \text{Tr} \mathcal{F}^2 + \frac{1}{4} \hat{\mathcal{A}} \hat{\mathcal{F}}^2 + (\text{total derivatives}) \right), \quad (2.15)$$

We see that in the case of two D-branes, the Chern-Simons coupling has two terms, one involving only  $U(1)$  fields and the other one which couples the  $U(1)$  and the  $SU(2)$  fields. In the present paper we will focus on the effect of the  $U(1)$  part.

## 2.2 Holographic realisation of chemical potentials

Holographic models encode *global* symmetries of the dual gauge theory in the form of *gauge* symmetries in the bulk theory, and these relations hold both for the closed as well as the open sectors of the string theory. So in particular, in the D8- $\overline{\text{D8}}$  system, there are two independent gauge theories living near the two boundaries of the flavour brane system, giving rise to  $U(N_f)_L$  and  $U(N_f)_R$  gauge symmetries, and these correspond to the global  $U(N_f) \times U(N_f)_R$  of the dual gauge theory.

In the low-temperature phase of the Sakai-Sugimoto model that we are interested in, the two branes are connected in the interior of the bulk space, and thus the gauge fields  $\mathcal{A}_M^L$  and  $\mathcal{A}_M^R$  are limits of a single gauge field living on the two connected branes. Therefore, one cannot independently perform gauge transformations on these two gauge fields, but is constrained to gauge transformations which, as  $z \rightarrow \pm\infty$ , act in a related way. Specifically, since near the boundary a large bulk gauge transformation acts as  $\mathcal{A}_{L/R} \rightarrow g_{L/R} \mathcal{A}_{L/R} g_{L/R}^{-1}$ , then clearly if  $g_L = g_R$  any state (and in particular the trivial vacuum  $\mathcal{A} = 0$ ) is invariant under the vectorial transformations, i.e. those transformations for which  $g_L = g_R$ . Hence it means that the vector-like symmetry is unbroken in this model.

The correspondence between the bulk gauge field and the source and global symmetry current of the dual gauge theory is encoded in the asymptotic behaviour

---

<sup>4</sup>For comparison, our  $\hat{\alpha}$  corresponds to 4/3 times  $\alpha$  used in [5].

of the former. More precisely, the bulk gauge field  $\mathcal{A}_M(z, x^\mu)$  behaves, near the boundary and in the  $\mathcal{A}_z = 0$  gauge, as

$$\mathcal{A}_n(x^\mu, z) \rightarrow a_n(x^\mu) \left(1 + \mathcal{O}(z^{-2/3})\right) + \rho_n(x^\mu) \frac{1}{z} \left(1 + \mathcal{O}(z^{-2/3})\right). \quad (2.16)$$

Here  $a_n(x^\mu)$  describes non-normalisable behaviour of the field, and is interpreted as a source in a dual field theory action of the form

$$\int d^4x a_n(x^\mu) J^n(x^\mu), \quad (2.17)$$

while  $\rho_n(x^\mu)$  is proportional to the expectation value of the current  $J_n(x^\mu)$ . Therefore, adding a chemical potential to the field theory corresponds to adding a source for  $J^0$ , which implies the boundary condition for the holographic gauge field  $\mathcal{A}_n(x) = \mu \delta_{n0}$ .

For the Sakai-Sugimoto model, the bulk field  $\mathcal{A}_m$  living on the D8-branes has *two* asymptotic regions, corresponding to each brane, and hence there are two independent chemical potentials  $\mu_L$  and  $\mu_R$  which can be separately turned on. Instead of left and right chemical potentials one often introduces vectorial and axial potentials, defined respectively as  $\mu_V = \frac{1}{2}(\mu_L + \mu_R)$  and  $\mu_A = \frac{1}{2}(\mu_L - \mu_R)$ . The vectorial and axial chemical potentials for the  $U(1)$  subgroup of the  $U(2)$  gauge group on the two D8-branes correspond to the baryonic and axial chemical potential in the dual gauge theory, while the non-abelian  $SU(2)$  chemical potentials are mapped to the vectorial and axial isospin potentials.

In this paper we will be interested only in *axial* chemical potentials. Our computations will mainly be concerned with the  $U(1)$  subgroup, since the instability which leads towards the spatially modulated phase in the  $U(1)$  subgroup is present in the same form in the  $U(1)$  subgroup of an isospin  $SU(2)$  group, leading to the instability of homogeneous configuration for the isospin chemical potential as well.

Our starting point is the *homogeneous* solution [6] in the  $\mathcal{A}_z = 0$  gauge. For the configuration to describe an axial chemical potential one needs to turn on only the  $\mathcal{A}_0(z)$  component, and look for odd, non-normalisable solutions to the equations of motion (3.2). It is not hard to see that with this simple ansatz the Chern-Simons contribution to the equations of motion vanishes, and the solution to the equation of motion is given by

$$\mathcal{A}_0(z) = \frac{2}{\pi} \mu_A \arctan z. \quad (2.18)$$

Just as in the chiral Lagrangian, there is no potential generated on moduli space [8], and the result of the axial potential is simply a non-vanishing axial density. The value of this density is easily read off using (2.16) to be  $\rho_A = 2\mu_A/\pi$ . This same solution can also be trivially embedded in the  $U(1)$  subgroup of the  $SU(2)$  isospin group. In this case however, as explained in [8], the odd  $\mathcal{A}_0(z)$  configuration in the  $\mathcal{A}_z = 0$  gauge is equivalent (by a global  $SU(2)$  rotation) to a system with a vectorial chemical potential and a non-trivial pion condensate.



### 3 The spatially modulated phase

We have seen in the previous section that turning on the axial chemical potential in Sakai-Sugimoto model requires finding a non-normalisable spatially homogeneous solution for the  $U(1)$  field  $\mathcal{A}_0$ , which is an *odd* function in the holographic direction. The asymptotic values of  $\mathcal{A}_0$  correspond to the values of the chemical potentials in the dual gauge theory.

As mentioned in the introduction, the work of Domokos and Harvey [3] and Nakamura, Ooguri and Park [2, 4] has shown that in Maxwell theory with a Chern-Simons coupling turned on, a constant electric field is *unstable* against decay to a spatially modulated phase, in which a magnetic field transverse to the direction of the initial electric field is switched on. Since the configuration with non-vanishing axial chemical potential (2.18) amounts to having a non-vanishing electric field in the bulk, we expect that an instability similar to that found by the aforementioned authors should be present here. In the present section we will analyse the Sakai-Sugimoto model at zero temperature with non-zero axial chemical potential, show that for sufficiently large values of that potential a new ground state appears, and determine that it has lower energy than the homogeneous vacuum.

#### 3.1 Equations of motion

Let us begin by writing the effective 5-dimensional action for the case of a single flavour  $N_f = 1$ , obtained after we integrate out the fields on the four sphere  $S^4$ , for the case of the single D8- $\overline{\text{D8}}$  brane,

$$S_{\text{YM}} + S_{\text{CS}} = -\frac{\kappa}{2} \int d^4x dz \sqrt{-g} \mathcal{F}^{mn} \mathcal{F}_{mn} + \frac{\alpha}{4} \epsilon^{\ell mnpq} \int d^4x dz \mathcal{A}_\ell \mathcal{F}_{mn} \mathcal{F}_{pq}. \quad (3.1)$$

The equations of motion following from this action read

$$\begin{aligned} \sqrt{-g} [g^{00} g^{zz} \partial_0 \mathcal{F}_{0z} + g^{xx} g^{zz} \partial_i \mathcal{F}_{iz}] + \frac{3}{2} \frac{\alpha}{\kappa} \epsilon^{ijk} \mathcal{F}_{0i} \mathcal{F}_{jk} &= 0, \\ \partial_z [\sqrt{-g} g^{zz} g^{00} \mathcal{F}_{z0}] + \sqrt{-g} g^{00} g^{xx} \partial_i \mathcal{F}_{i0} - \frac{3}{2} \frac{\alpha}{\kappa} \epsilon^{ijk} \mathcal{F}_{zi} \mathcal{F}_{jk} &= 0, \\ \partial_z [\sqrt{-g} g^{zz} g^{xx} \mathcal{F}_{zi}] + \sqrt{-g} (g^{xx})^2 \partial_j \mathcal{F}_{ji} + \sqrt{-g} g^{00} g^{xx} \partial_0 \mathcal{F}_{0i} \\ + \frac{3}{2} \frac{\alpha}{\kappa} \epsilon^{ijk} \mathcal{F}_{z0} \mathcal{F}_{jk} - \frac{3}{\kappa} \epsilon^{ijk} \mathcal{F}_{zj} \mathcal{F}_{0k} &= 0. \end{aligned} \quad (3.2)$$

Here we have split the five-dimensional bulk indices as  $m = (i = (1, 2, 3), 0, z)$  and we have assumed that the general diagonal five-dimensional effective metric  $g_{mn}$  depends only on the  $z$  coordinate and has symmetry  $g_{11} = g_{22} = g_{33} = g_{xx}$  (valid for the Sakai-Sugimoto system).

It is important to note that the variation of the action (3.1) leads to a boundary term, which, after one uses the Bianchi identity  $\partial_m \mathcal{F}_{pq} + \partial_q \mathcal{F}_{mp} + \partial_p \mathcal{F}_{qm} = 0$ , reads

$$\delta S_{\text{bdy}} = - \int d^4 x dz \partial_m \left[ \delta \mathcal{A}_\ell \left( 2\kappa \sqrt{-g} \mathcal{F}^{m\ell} + \alpha \epsilon^{\ell mnpq} \mathcal{A}_n \mathcal{F}_{pq} \right) \right]. \quad (3.3)$$

Therefore, when  $\delta \mathcal{A}_\ell$  does not vanish, one has to add a boundary term to the action in order to ensure that there are no boundary contributions to the equations of motion (see e.g. [13] for a discussion in related context). This is important when we consider the system at constant density. In the appendix we discuss this issue in more detail, and give the corresponding boundary term for the antipodal embedding of D8- $\overline{\text{D8}}$  branes.

### 3.2 The abelian ansatz

To describe a spatially modulated phase, our starting point is the ansatz

$$\mathcal{A}_0 = f(z, \vec{x}), \quad \vec{\mathcal{A}} = \vec{\mathcal{A}}(z, \vec{x}), \quad (3.4)$$

where  $\vec{\mathcal{A}}$  are in the spatial directions of the boundary. We will work in the gauge  $\mathcal{A}_z = 0$ . Furthermore, we only want to turn on the chemical potential for the axial currents and insist that the spatially modulated phase is spontaneously generated (i.e. without introducing any kind of sources). Hence we impose normalisable boundary conditions on the fields  $\vec{\mathcal{A}}$ , while similar to the homogeneous case we impose that  $\mathcal{A}_0$  is non-normalisable, and tends to opposite constants at the two ends of the D8-brane system,

$$\vec{\mathcal{A}}(z = \pm\infty) = 0, \quad \mathcal{A}_0(z = \pm\infty) = \pm\mu_A. \quad (3.5)$$

For this ansatz (3.4) the full non-linear equations of motion (3.2) become<sup>5</sup>

$$\sqrt{-g} g^{xx} g^{zz} \partial_z (\nabla \cdot \vec{\mathcal{A}}) - 3 \frac{\alpha}{\kappa} \vec{\mathcal{E}} \cdot \vec{\mathcal{B}} = 0, \quad (3.6)$$

$$\partial_z \left[ \sqrt{-g} g^{zz} g^{00} \partial_z f \right] - \sqrt{-g} g^{00} g^{xx} (\nabla \cdot \vec{\mathcal{E}}) - 3 \frac{\alpha}{\kappa} (\partial_z \vec{\mathcal{A}}) \cdot \vec{\mathcal{B}} = 0, \quad (3.7)$$

$$\partial_z \left[ \sqrt{-g} g^{zz} g^{xx} \partial_z \vec{\mathcal{A}} \right] - \sqrt{-g} (g^{xx})^2 \nabla \times \vec{\mathcal{B}} + 3 \frac{\alpha}{\kappa} \left[ (\partial_z f) \vec{\mathcal{B}} - \partial_z \vec{\mathcal{A}} \times \vec{\mathcal{E}} \right] = 0. \quad (3.8)$$

In these equations,  $\vec{\mathcal{E}} = \mathcal{F}_{0i} \hat{x}^i = -\nabla f$  and  $\vec{\mathcal{B}} = \frac{1}{2} \epsilon_{ijk} \mathcal{F}_{jk} \hat{x}^i = \nabla \times \vec{\mathcal{A}}$  are the (bulk) transverse electric and magnetic field associated to  $f$  and  $\vec{\mathcal{A}}$ .

A simple ansatz that solves these equations is to impose

$$\vec{\mathcal{E}} = 0, \quad \vec{\mathcal{B}} = k \vec{\mathcal{A}}, \quad (3.9)$$

---

<sup>5</sup>In order to compare our normalisation of the Chern-Simons coupling  $\alpha$  with [5], note that equation (6) of that paper contains a typo: the coefficient  $\alpha$  should read  $\alpha/6$ .

where  $k = \pm|\vec{k}|$  and  $\vec{k}$  is the spatial momentum. This way the equation (3.6) is automatically satisfied and the equation (3.7) can be integrated. The gauge field consistent with this ansatz can be written as

$$\mathcal{A}_0 = f(z), \quad \vec{\mathcal{A}} = \vec{\eta}_1 h(z) \cos(\vec{k} \cdot \vec{x}) + \vec{\eta}_2 h(z) \sin(\vec{k} \cdot \vec{x}), \quad (3.10)$$

where  $\vec{\eta}_1, \vec{\eta}_2$  are polarisation vectors satisfying

$$\vec{\eta}_1 \times \vec{k} = k \vec{\eta}_2, \quad \vec{k} \times \vec{\eta}_2 = k \vec{\eta}_1. \quad (3.11)$$

For simplicity we choose  $\vec{k} = k \hat{x}_1$  so that the polarisation vectors reduce to  $\vec{\eta}_1 = \hat{x}_2$ ,  $\vec{\eta}_2 = -\hat{x}_3$  where  $h(z)$  is a function that vanishes at  $z \rightarrow \pm\infty$ . The equations (3.7) and (3.8) take the form

$$M_{KK}^2 K_z \partial_z f = \tilde{\rho} - \frac{3\alpha}{2\kappa} k h^2, \quad (3.12)$$

$$M_{KK}^4 K_z \partial_z [K_z \partial_z h] - M_{KK}^2 K_z^{2/3} k^2 h + 3 \frac{\alpha}{\kappa} k h \left[ \tilde{\rho} - \frac{3\alpha}{2\kappa} k h^2 \right] = 0, \quad (3.13)$$

where  $\tilde{\rho}$  is an integration constant,  $K_z = 1 + z^2$  and  $M_{kk}$  is defined in (2.2). Equations (3.12) and (3.13) form the system that determines the new vacuum. In order to solve numerically this system it is convenient to introduce dimensionless variables  $\hat{f}, \hat{h}, \hat{k}$  and  $\hat{\rho}$  defined by

$$f = \bar{\lambda} M_{KK} \hat{f} \quad h = \bar{\lambda} M_{KK} \hat{h} \quad k = M_{KK} \hat{k} \quad , \quad \tilde{\rho} = \bar{\lambda} M_{KK}^3 \hat{\rho}, \quad (3.14)$$

with  $\bar{\lambda} = \lambda/(27\pi)$ . Then equations (3.12) and (3.13) can be written as

$$K_z \partial_z \hat{f} = \hat{\rho} - \frac{\hat{\alpha}}{2} \hat{k} \hat{h}^2, \quad (3.15)$$

$$K_z \partial_z [K_z \partial_z \hat{h}] + \left[ \hat{\alpha} \hat{k} \hat{\rho} - K_z^{2/3} \hat{k}^2 \right] \hat{h} - \frac{\hat{\alpha}^2}{2} \hat{k}^2 \hat{h}^3 = 0. \quad (3.16)$$

To determine the physical meaning of the integration constant  $\hat{\rho}$ , we recall that the charge density of the dual axial current  $J_\mu^A$  is computed using the AdS/CFT dictionary as

$$\rho_A \equiv \langle J_0^A \rangle_\pm \sim \lim_{z \rightarrow \infty} z^2 \partial_z \mathcal{A}_0 + \lim_{z \rightarrow -\infty} z^2 \partial_z \mathcal{A}_0. \quad (3.17)$$

From the asymptotic behaviour  $\hat{h}(z) \sim \alpha_0/z + \dots$ , which can be obtained by perturbatively solving (3.16), one deduces that the function  $\hat{h}(z)$  does not contribute to the charge so  $\hat{\rho}$  is indeed the charge density of the dual axial current (up to a constant). However, this does not mean that the charge density is the same as in the homogeneous case. The reason is that the chemical potential is determined via

$$\mu_A = \frac{1}{2} \left( \lim_{z \rightarrow \infty} \mathcal{A}_0 - \lim_{z \rightarrow -\infty} \mathcal{A}_0 \right) = \frac{1}{2} \int_{-\infty}^{\infty} dz \partial_z \mathcal{A}_0(z). \quad (3.18)$$

Therefore, we see that the constant  $\alpha_0$  *does* contribute to the value of the chemical potential, and hence modifies it in a nontrivial way so as to give a new relation between the chemical potential  $\mu_A$  and axial charge  $\rho_A$ . We will see this explicitly in the next section (see figure 3).

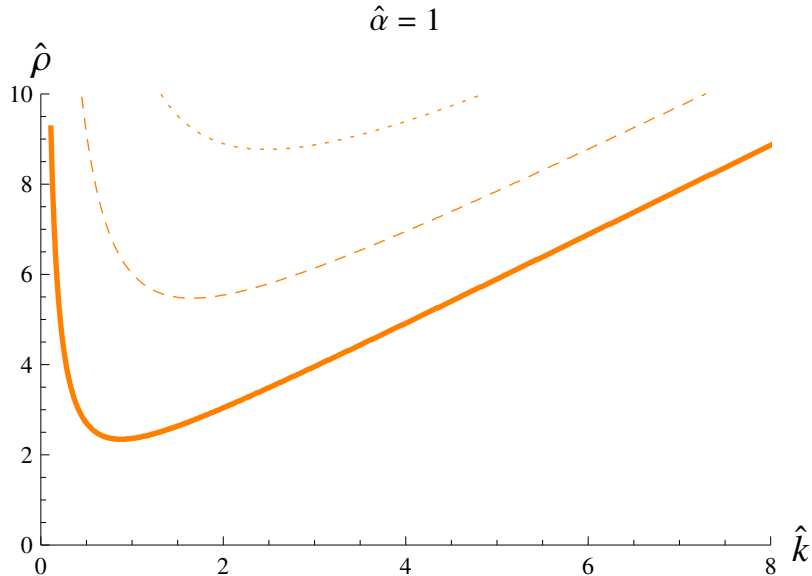


**Figure 1.** Result of the stability analysis in the Maxwell-Chern-Simons system. The curve shows the values of  $\hat{\rho}$  and  $\hat{k}$  for which an instability sets in. From this analysis one finds  $\rho_{\text{crit}} \approx 2.35$ , and the corresponding mode is vectorial. The dashed and dotted curves correspond to additional instabilities of axial and vectorial nature respectively, which set in at higher values of the density.

### 3.3 Analysis of the ground state

In order to find the spatially modulated phase (3.10) we need to solve equation (3.13) for  $h(z)$  and then use this solution when determining  $f(z)$  using equation (3.12). Equation (3.13) can be solved numerically using a shooting method.

Before presenting our numerical solutions, let us note that equations (3.13) and (3.12) have three free parameters: the Chern-Simons coupling  $\alpha$  defined in (2.12), the wave number  $k$  which sets the frequency of the spatial modulation, and the charge density of the dual current  $\tilde{\rho}$  which appears as an integration constant in equation (3.12). The wave number  $k$  will be kept free, i.e. we solve the equation for various values of this parameter. In string theory the constant  $\alpha$  has a fixed value, but one might consider a more phenomenological attitude in which  $\alpha$  is allowed to take on any value. In this section we will set  $\alpha$  to its string theory value, so that  $\hat{\alpha} = 1$ . The reason is that in Maxwell-Chern-Simons theory, which we discuss in this section, the actual value of coupling is not really relevant: for any  $\alpha$ , a non-homogeneous state can be made to appear since one can always make the chemical potential large enough. The situation is however different when dealing with the DBI action, which we discuss in §4.

Because we do not want to introduce any external sources in the boundary theory, we are looking for *normalisable* solutions of the equation (3.13). This means that,

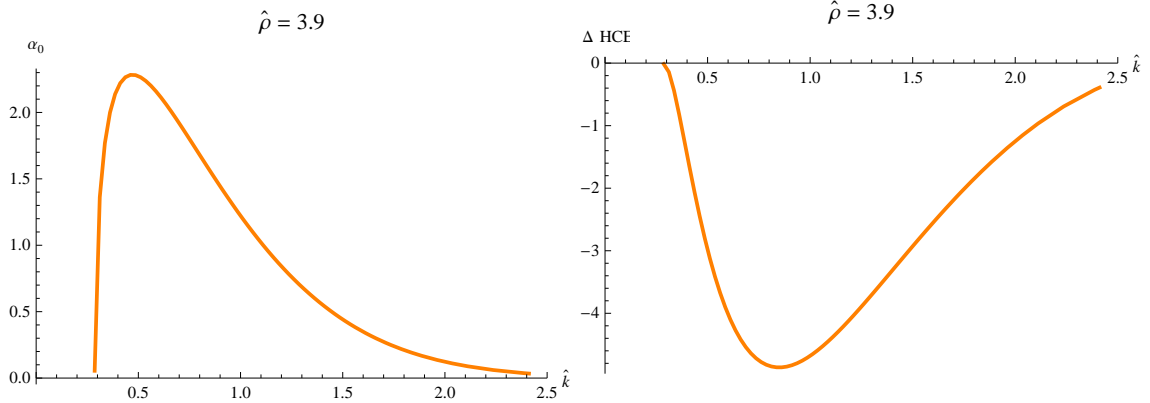


**Figure 2.** The charge density of the non-homogeneous solution, as well as the energy difference with respect to the homogeneous vacuum, as a function of the momentum. These plots show the range of momentum values  $(k_{\min}, k_{\max})$  for which non-homogeneous solutions exist. Both plots are made for a charge density  $\hat{\rho} = 3.9$ .

even though (3.13) is a second order equation, there is only one undetermined parameter,  $\alpha_0$ , which governs the behaviour of the function  $h(z)$  near infinity. By expanding the equation (3.13) around  $\pm\infty$  it is easy to see that  $h$  behaves as  $h(z) \sim \alpha_0/z + \dots$ . Using the AdS/CFT dictionary we see that the constant  $\alpha_0$  is related to the expectation value of the dual current in the directions  $\vec{\eta}_1$  and  $\vec{\eta}_2$  on the boundary,

$$\begin{aligned} \langle J_{\vec{\eta}_1} \rangle &= \lim_{z \rightarrow \infty} z^2 \mathcal{F}_{\vec{\eta}_1 z} = \alpha_0 \cos(\vec{k} \cdot \vec{x}), \\ \langle J_{\vec{\eta}_2} \rangle &= \lim_{z \rightarrow \infty} z^2 \mathcal{F}_{\vec{\eta}_2 z} = \alpha_0 \sin(\vec{k} \cdot \vec{x}). \end{aligned} \quad (3.19)$$

If the current is vectorial, then the same values are obtained by taking the limit  $z \rightarrow \pm\infty$ , otherwise it is axial.

Next, we use a shooting method to numerically solve (3.13) for various values of charge densities  $\rho$  and momenta  $k$ . The first observation is that there is a critical value of the charge density (and corresponding potential) so that if the density is larger than  $\rho_{\text{crit}}$ , non-homogeneous solutions will exist. This critical value is best obtained using a linear analysis, looking for unstable modes in the homogeneous vacuum. A fluctuation with frequency  $\omega$  satisfies the linear truncation of (3.13) with an additional term proportional to  $\omega$  added. A marginally unstable mode is then obtained by solving for modes which have  $\omega = 0$ , i.e. modes satisfying the linear truncation of (3.13). Such modes occur for one-dimensional subspaces of the  $\rho - k$  plane. Figure 1 depicts the result of this analysis, which shows that there are various branches of unstable modes. More specifically, we have found that for any  $\hat{\rho} > \hat{\rho}_{\text{crit}} \approx 2.35$ , instabilities exist.

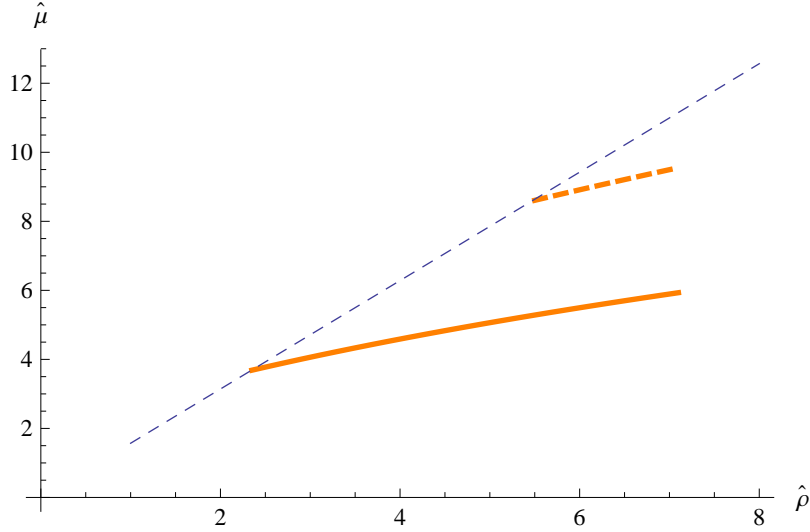


**Figure 3.** The chemical potential as a function of the charge density for the non-homogeneous ground state. The thick dashed line describes the higher-energy, axial branch of the solutions, which are meta-stable. The thin diagonal dashed line shows the relation  $\hat{\mu}_A = \pi\hat{\rho}_A/2$  for the homogeneous vacuum.

Corresponding to these instabilities are new ground states. For any momentum in the range  $[\hat{k}_{\min}(\hat{\rho}), \hat{k}_{\max}(\hat{\rho})]$ , where  $\hat{k}_{\min}$  and  $\hat{k}_{\max}$  are the two values of  $\hat{k}$  on a line of instability at fixed  $\hat{\rho}$ , we find non-homogeneous solutions of the non-linear equations. See figure (2) for an example at  $\hat{\rho} = 3.9$ . However, among all solutions for a given  $\hat{\rho}$ , there is only one momentum  $\hat{k} = \hat{k}_{\text{gs}}(\hat{\rho})$  for which the solution has minimal energy. Hence this value specifies the unique ground state for a given charge density or chemical potential. We should emphasise that when we determine the ground state, we have compared the homogeneous and non-homogeneous solutions at *fixed charge density*  $\hat{\rho}$ . In other words we are working in the *canonical ensemble*. One could also work in the grand canonical ensemble, comparing solutions at the same value of the chemical potential  $\hat{\mu}_A$ . The results which are obtained in that case are qualitatively the same as in the canonical ensemble, so we choose to present only the canonical ensemble results here.

The solutions describing ground state are uniquely specified by the value of the charge density  $\hat{\rho}$ . In other words, the parameters  $(\alpha_0, \hat{k}_{\text{gs}}, \hat{\mu}_A)$  specifying the ground state are all functions of the charge density  $\hat{\rho}$ . The dependence of the chemical potential on the charge density is plotted in figure 3, which also shows the relation between these two parameters in the homogeneous solution. We see that the relation is again (almost) linear in the non-homogeneous case, but for a given value of the charge density the chemical potential in the homogeneous case is larger than in the non-homogeneous case. The dependence of the momentum  $\hat{k}_{\text{gs}}$  on the density  $\hat{\rho}$  is

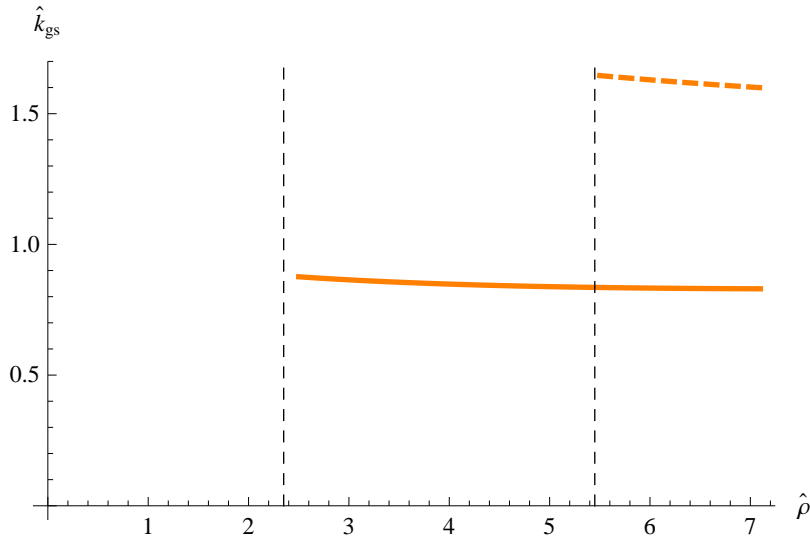


**Figure 4.** The momentum of the spatial modulation as a function of the charge density for the non-homogeneous ground state. The dashed line describes the higher energy, axial branch. Observe that the momentum is practically independent of the density.

shown in figure 4. Interestingly, we see that the momentum is almost independent of the charge density. It would be interesting to understand better the reason for this behaviour. To see if this is a consequence of the Maxwell approximation of the DBI action, we will examine this relation again in the nonlinear DBI case in the next section. Finally, the dependence of the constant  $\alpha_0$  on the density  $\hat{\rho}$  is shown in figure 5. As is visible from equation (3.19) this constant is equal to the amplitude of the current components  $J_{\eta_1}$  and  $J_{\eta_2}$ .

The difference between the free energies of the homogeneous and non-homogeneous configurations (see equation (6.5)) for fixed value of the charge density  $\rho$  is displayed in figure 6. As required, we see that when  $\hat{\rho} > \hat{\rho}_{\text{crit}}$ , the free energy of the non-homogeneous configuration is lower than the one of the homogeneous configuration, indicating that the system will settle in the new ground state. We also see that for large enough charge density,  $\hat{\rho} > 5.4$ , a new branch of solutions appears. While the first non-homogeneous branch is given by an even function  $h(z)$ , thus describing a *vectorial* current, the next branch is an odd function, describing an *axial* current. As the chemical potential is increased further, yet more branches occur, alternating between vectorial and axial. However, as is manifest from figure 6, all higher branches have higher values of the free energy, and thus correspond to excited states, not ground states.

Finally we should note that while the ground state is characterised by *vectorial* spatial components  $\eta_1$  and  $\eta_2$  of the current  $J$ , the charge density is always axial. This is a consequence of the fact that the integrand in (3.12) is an even function for

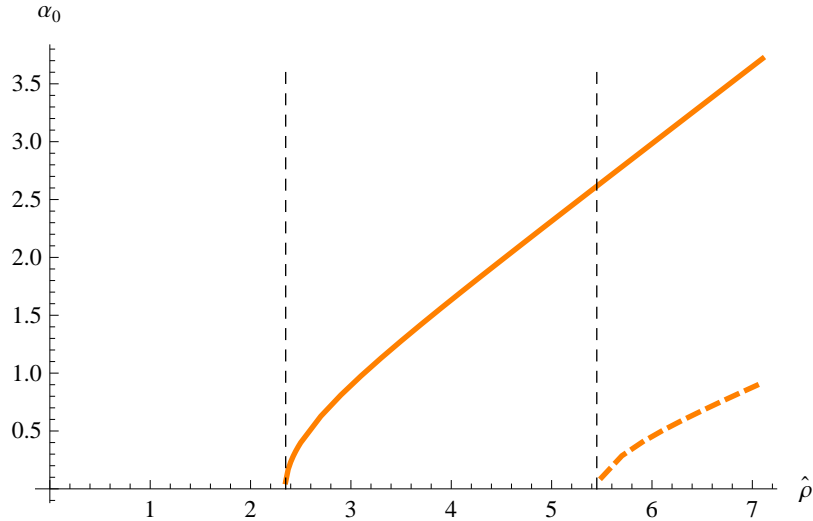


**Figure 5.** The amplitude of the expectation value of the currents  $\langle J_{\eta_1} \rangle$  or  $\langle J_{\eta_2} \rangle$  as a function of the density. The dashed curve is again the unstable axial branch.

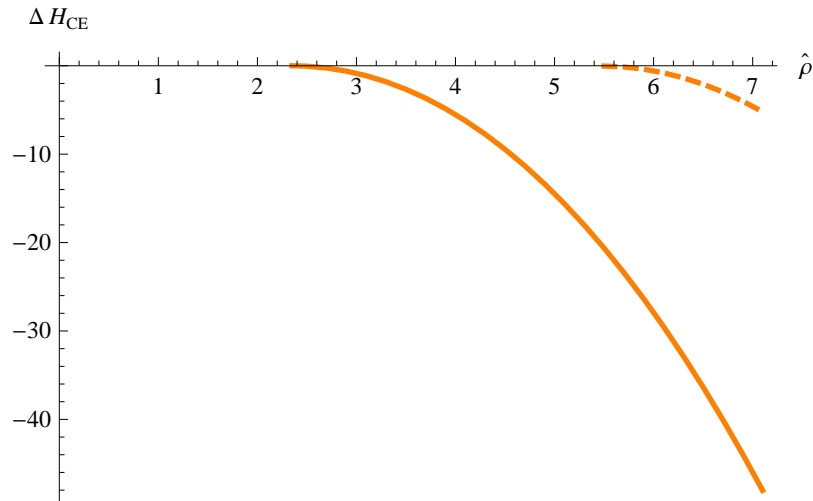


**Figure 6.** The difference between the free energies of the homogeneous and non-homogeneous configurations as a function of the charge density. The dashed line depicts the axial ground state, which clearly has higher energy and is therefore unstable.

any function  $h(z)$ .

In conclusion, we see that the Sakai-Sugimoto model predicts that, even at zero temperature, a non-trivial condensate of vector mesons forms for sufficiently large value of the axial chemical potential  $\mu_A$ . This condensate is non-homogeneous, and its spatial modulation has a momentum vector which is almost constant as a function of the chemical potential. These results complement those in deconfined phase obtained by [5].



## 4 Spatially modulated phase for the DBI action

In the Maxwell-Chern-Simons theory, an instability towards a new ground state of the type found in the previous section will always occur, independent of the strength of the Chern-Simons coupling. This is simply because the electric field (and hence the axial chemical potential  $\mu_A$ ) can be made arbitrarily large. However, given the fact that the Chern-Simons term is of order  $\lambda^{-1}$  with respect to the Maxwell term, the fields in this new ground state are necessarily of order  $\lambda$ . The solution found in the previous section can therefore not be seen as an approximate solution to the full DBI system, since the truncation that leads to the Maxwell action assumes that  $\lambda$  is small. Re-analysing the computation for the DBI action may thus yield qualitatively new results.<sup>6</sup>

Furthermore, in the full DBI system, there is an upper bound on the electric field, which may prevent the instability from setting in [5]. A final reason to repeat the previous analysis for the DBI-Chern-Simons action is to examine the question whether the non-linearities of the DBI action modify the values of the ground state momentum  $k_{\text{gs}}$ , perhaps making it dependent on the charge density.

Our starting point is the DBI action for the D8- $\overline{\text{D8}}$  system, after integration over the  $S^4$  (on which none of the fields which are turned on depend),

$$S_{\text{DBI}} = - \int d^4x dz \gamma(z) \sqrt{-E} \quad (4.1)$$

where

$$E = \det(E_{mn}) \quad , \quad E_{mn} = g_{mn} + \beta(z) \mathcal{F}_{mn} \quad , \quad (4.2)$$

with

$$\begin{aligned} \gamma(z) &= V_{S^4} \mu_8 e^{-\phi} a(z)^{5/2} b(z)^2 = \frac{\bar{\lambda}^3 N_c}{\pi^2} K_z^{-1/3} \quad , \\ \beta(z) &= \frac{2\pi\alpha'}{a(z)} = \frac{1}{2\lambda} K_z^{1/6} \quad . \end{aligned} \quad (4.3)$$

Here  $g_{mn}$  is the effective 5-d metric defined in (2.10) and  $a(z)$  and  $b(z)$  are given by

$$a(z) = \frac{8}{27} M_{KK} R^3 K_z^{-1/6} \quad , \quad b(z) = \frac{2}{3} M_{KK} R^3 K_z^{1/6} \quad . \quad (4.4)$$

This action is coupled to the Chern-Simons term

$$S_{\text{CS}} = \frac{\alpha}{4} \epsilon^{\ell mnpq} \int d^4x dz \mathcal{A}_\ell \mathcal{F}_{mn} \mathcal{F}_{pq} \quad . \quad (4.5)$$

The coupling  $\alpha$  is defined to be  $\alpha = \hat{\alpha} N_c / (24\pi^2)$  with  $\hat{\alpha}$  fixed in string theory to  $\hat{\alpha} = 1$ . However, since we are interested in investigating the nature of the instability we will relax this condition and consider an arbitrary  $\hat{\alpha}$ .

---

<sup>6</sup>Note that because the momentum scale  $k$  of the spatial modulation is set by  $M_{kk}$  (as follows from (3.14)), higher-derivative corrections can be ignored when  $l_s M_{kk}$  is sufficiently small.

The action variation leads to the DBI-CS equations

$$\partial_m \left( \frac{\gamma\beta}{2} \sqrt{-E} E^{(\ell,m)} \right) + \frac{3}{4} \alpha \epsilon^{\ell m n p q} \mathcal{F}_{mn} \mathcal{F}_{pq} = 0, \quad (4.6)$$

and the boundary term

$$\delta S_{\text{bdy}} = - \int d^4x dz \partial_m \left[ \left( \frac{\gamma\beta}{2} \sqrt{-E} E^{(\ell,m)} + \alpha \epsilon^{\ell m n p q} \mathcal{A}_n \mathcal{F}_{pq} \right) \delta \mathcal{A}_\ell \right]. \quad (4.7)$$

Here we have introduced the antisymmetric tensor  $E^{(\ell,m)} = E^{\ell m} - E^{m\ell}$  where  $E^{\ell m}$  is defined by  $E^{\ell m} E_{mn} = \delta_n^\ell$ .

For the ansatz (3.10), the nonzero components of  $E^{(\ell,m)}$  can be written as

$$\begin{aligned} E^{(z,0)} &= - \frac{2\beta g^{zz} g^{00} \partial_z f}{1 + g^{zz} g^{00} \beta^2 (\partial_z f)^2 + g^{zz} g^{xx} (\partial_z h)^2}, \\ E^{(z,i)} &= - \frac{2\beta g^{zz} g^{xx} \partial_z A_i}{1 + g^{zz} g^{00} \beta^2 (\partial_z f)^2 + g^{zz} g^{xx} (\partial_z h)^2}, \\ E^{(1,i)} &= - \frac{2\beta (g^{xx})^2 \partial_1 A_i}{1 + (g^{xx})^2 \beta^2 k^2 h^2}. \end{aligned} \quad (4.8)$$

Using these results the DBI-CS equations can be written in a form which puts all modifications due to the DBI action in a single function  $Q(z)$ : the equation (3.12) becomes

$$Q(z) K_z \partial_z \hat{f} = \hat{\rho} - \frac{\hat{\alpha}}{2} \hat{k} \hat{h}^2, \quad (4.9)$$

while the analogue of equation (3.13) for  $h(z)$  now reads

$$Q(z) K_z \partial_z \left[ Q(z) K_z \partial_z \hat{h} \right] + \left[ \hat{\alpha} \hat{k} \hat{\rho} - K_z^{-2/3} \hat{k}^2 \right] \hat{h} - \frac{\hat{\alpha}^2}{2} \hat{k}^2 \hat{h}^3 = 0. \quad (4.10)$$

The function  $Q(z)$  itself is given by

$$Q(z) = \frac{\sqrt{1 + \frac{1}{4K_z} \left[ \hat{k}^2 \hat{h}^2 + K_z^{-2/3} \left( \hat{\rho} - \frac{\hat{\alpha}}{2} \hat{k} \hat{h}^2 \right)^2 \right]}}{\sqrt{1 + \frac{1}{4} K_z^{1/3} (\partial_z \hat{h})^2}} \quad (4.11)$$

and we used again the dimensionless variables introduced in (3.14).

#### 4.1 Stability analysis

Before solving the non-linear equation (4.10), it is useful to analyse again possible instabilities in the fluctuation spectrum, in particular in order to see how they depend on the Chern-Simons coupling  $\alpha$ . Similar to the discussion for the Maxwell case, we can find unstable modes by solving for  $h(z)$  in the linearised version of (4.10). Results for two values of  $\hat{\alpha}$  are given in figure 7. One observes that the number of

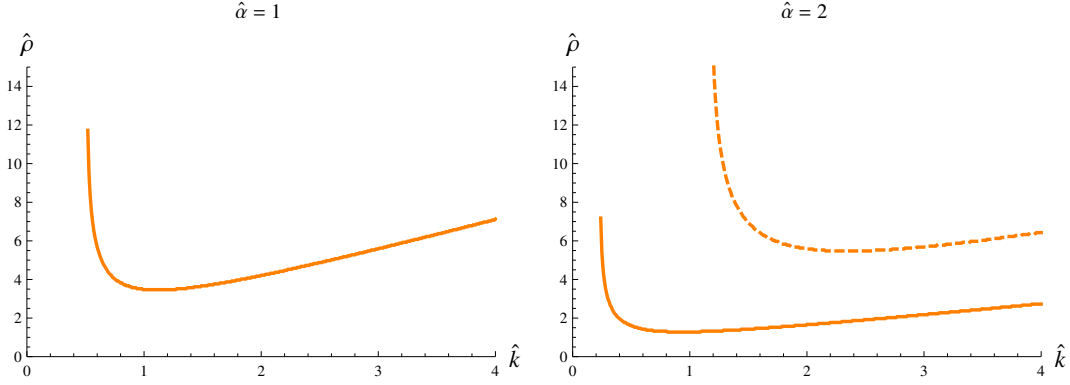


**Figure 7.** The relation between  $\rho$  and  $k$  for the unstable mode of the DBI system, for two values of the Chern-Simons coupling:  $\alpha = 1$  for the left panel and  $\alpha = 2$  for the right panel.

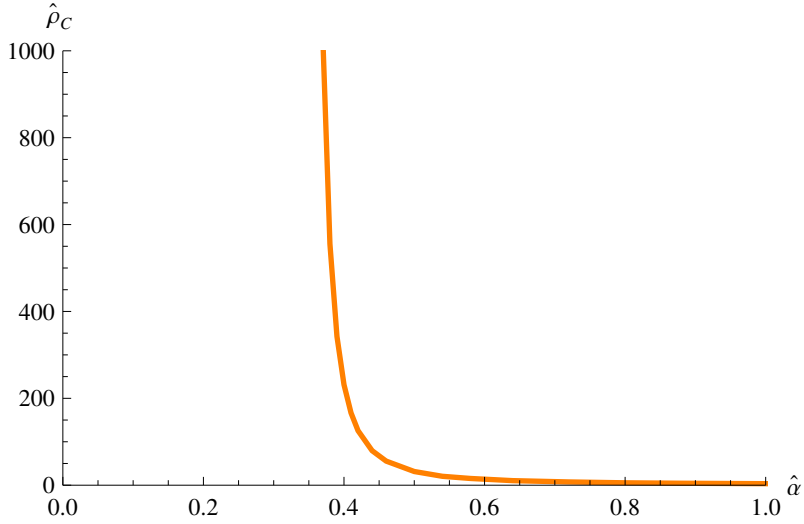


**Figure 8.** The relation between the critical value of the density and the Chern-Simons parameter  $\hat{\alpha}$ . The critical density diverges as  $\hat{\alpha} \rightarrow 1/3$ .

solutions which survive from the Maxwell truncation is determined by the Chern-Simons coupling, and larger values typically make the curves shift to the bottom left of the graph. For  $\hat{\alpha} = 1$  (the value used in the Maxwell case), the critical density is now found to be  $\hat{\rho}_{\text{crit}} \approx 3.46$ , i.e. larger than in the Maxwell case.

From this instability analysis one can also find the minimum value of  $\hat{\alpha}$  for which an instability is possible at all. Figure 8 shows the critical density  $\hat{\rho}_{\text{crit}}$  as a function of  $\hat{\alpha}$ . This plot agrees with a divergence as  $\hat{\alpha} \rightarrow 1/3$ , just as in [5], indicating that there is no instability in the system when  $\hat{\alpha}$  takes on smaller values. For such values, the non-linearities of the DBI action eliminate the instabilities visible in the Maxwell truncation.

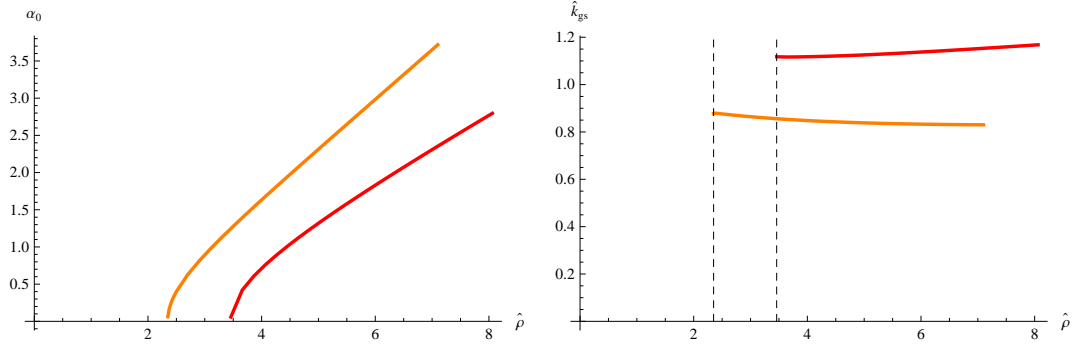


**Figure 9.** Summary of the DBI analysis, with red (dark) curves depicting the DBI results and the Maxwell result is given in orange (light) for comparison. The left panel shows the expectation value of the current  $\langle J \rangle$  as a function of the density. The critical density has now shifted to  $\hat{\rho}_{\text{crit}} \approx 3.46$ . The right panel shows that the momentum vector is still practically independent of  $\hat{\rho}$ , but has also changed value.

## 4.2 Ground state: Maxwell versus DBI

Finally, we present the analysis of the non-homogeneous ground state in the DBI case. The logic of obtaining it is again the same as in the Maxwell case, so we will not dwell on it. We have already commented on the fact that the critical density is now substantially larger. This is again seen explicitly in the plot of the current expectation value  $\langle J_1 \rangle$  (or  $\langle J_2 \rangle$ ), given in the left panel of figure 9.

As far as the spatial modulation itself is concerned, we find from this analysis that the momentum vector  $k_{\text{gs}}$  for which the non-homogeneous ground state has minimal energy is now somewhat higher than in the Maxwell case. This is depicted in the right panel of figure 9. Nevertheless, it is still practically independent of the density.

Numerically, the instability at  $\hat{\rho}_{\text{crit}} \approx 3.46$  corresponds, using  $M_{KK} = 949 \text{ MeV}$  and  $\lambda = 16.6$  [6], to a physical density of  $\rho_{\text{crit}} = 4\kappa\tilde{\rho} \approx 0.79 N_c \text{ fm}^{-3}$  when  $N_f = 2$  (this is close to the numerical result of [5] up to somewhat puzzling factors of two).

## 5 Discussion and open questions

We have analysed the effect of an axial chemical potential in the Sakai-Sugimoto model in the low-temperature phase where chiral symmetry is broken. We have found that for sufficiently large chemical potential, a vectorial condensate forms, which is spatially modulated with a momentum vector which is practically independent of the potential or charge density.

The results persist beyond the Maxwell truncation for the DBI action as well. The main difference between the two is that critical density and spatial modulation momentum take on larger values in the DBI case. The non-linearities thus in a

sense stabilise the homogeneous phase. It would be interesting to understand if the instabilities of the type we find persist if further non-linearities due to gravity back-reaction are included.

It would also be interesting to understand if the new phase which we find occurs in other QCD-like theories, and in particular in QCD itself. The analysis of [12] does not find this phase, so it is worthwhile to analyse other (holographic and non-holographic) models and isolate more carefully which feature of the theory is responsible for the existence of the new phase. It would also be interesting to understand how robust is our finding that the spatial modulation is almost independent of the value of the charge density, especially since in the large- $N_c$  analysis for the quark chemical potential [1], the momentum is proportional to the chemical potential  $k_{\text{DGR}} \sim \mu_V$ .

Putting together our results with those of Park and Ooguri [5], we can construct a large part of the phase diagram of the Sakai-Sugimoto model in the presence of an axial chemical potential. We see that both in the confining and non-confining (and chirally symmetric) phases at large enough values of the axial chemical potential a second order phase transition to a new non-homogeneous phase appears. To complete the phase diagram it would be interesting to study the deconfinement in the presence of the non-homogeneous condensate, and see if and how it modifies the deconfinement temperature. For related work in other models see e.g. [14].

Finally, the chemical potential analysed in this paper can be embedded in the context discussed in [8]. The question then arises how the homogeneous (but non-isotropic) condensate found there competes with the non-homogeneous condensate found in the present paper. We will return to this question in a future publication.

## Acknowledgements

We thank Ofer Aharony and Cobi Sonnenschein for correspondence. This work was sponsored in part by STFC Rolling Grant ST/G000433/1.

## 6 Appendix: The Hamiltonian

### 6.1 Maxwell truncation

Here we present the detailed formulas for the Hamiltonian associated with the Chern-Simons action, taking special care about the surface terms which are present for the D8- $\overline{\text{D8}}$  system.

Our starting point is the Lagrangian density of the Maxwell-Chern-Simons action of (3.1), where we split the space and time indices,

$$\mathcal{L} = -\kappa \left[ \mathcal{F}^{0a} \mathcal{F}_{0a} + \frac{1}{2} \mathcal{F}^{ab} \mathcal{F}_{ab} \right] + \frac{\alpha}{4\sqrt{-g}} \epsilon^{0abcd} [\mathcal{A}_0 \mathcal{F}_{ab} \mathcal{F}_{cd} + 4\mathcal{F}_{0a} \mathcal{A}_b \mathcal{F}_{cd}] \quad (6.1)$$

The conjugate momentum associated to  $\partial_0 \mathcal{A}_a$  is given by

$$\Pi^a = \frac{\partial \mathcal{L}}{\partial(\partial_0 \mathcal{A}_a)} = -2\kappa \mathcal{F}^{0a} + \frac{\alpha}{\sqrt{-g}} \epsilon^{0abcd} \mathcal{A}_b \mathcal{F}_{cd}, \quad (6.2)$$

so that the Hamiltonian takes the form

$$\begin{aligned} H_{\text{M-CS}} = \kappa \int d^3 \bar{x} dz \left\{ \sqrt{-g} \left[ -\mathcal{F}^{0a} \mathcal{F}_{0a} + \frac{1}{2} \mathcal{F}^{ab} \mathcal{F}_{ab} \right] + \partial_a [\sqrt{-g} \Pi^a \mathcal{A}_0] \right. \\ \left. - 2 \left[ \partial_a (\sqrt{-g} \mathcal{F}^{a0}) + \frac{3\alpha}{8\kappa} \epsilon^{0abcd} \mathcal{F}_{ab} \mathcal{F}_{cd} \right] \mathcal{A}_0 \right\}. \end{aligned} \quad (6.3)$$

The first two terms in the above Hamiltonian belong to the bulk part  $H_{\text{bulk}}$ , the third term is a surface term, i.e. a boundary Hamiltonian  $H_{\text{bdy}}$ , while the terms in the last line vanish, since it is just the zeroth component of the Maxwell-Chern-Simons equations of motion.

Using the Maxwell-CS equations of motion and the ansatz (3.10), the canonical momentum (6.2) reduces to

$$\Pi^i = 0, \quad \Pi^z = \frac{2\kappa}{\sqrt{-g}} \left[ -\tilde{\rho} + \frac{\alpha}{2\kappa} k h^2 \right], \quad (6.4)$$

and the Hamiltonian becomes  $H_{\text{M-CS}} = H_{\text{bulk}} + H_{\text{bdy}}$  with

$$H_{\text{bulk}} = \mathcal{H} \int dz \left[ \frac{1}{K_z} (\hat{\rho} - \frac{\hat{k}}{2} \hat{h}^2)^2 + K_z (\partial_z \hat{h})^2 + K_z^{-1/3} \hat{k}^2 \hat{h}^2 \right], \quad (6.5)$$

$$H_{\text{bdy}} = 2\kappa V_x \left[ \left( -\tilde{\rho} + \frac{\alpha}{2\kappa} k h^2 \right) f \right]_{z \rightarrow -\infty}^{z \rightarrow \infty} = -4\mathcal{H} \hat{\rho} \hat{\mu}_A, \quad (6.6)$$

where  $\mathcal{H} = M_{\text{KK}}^4 V_x \bar{\lambda}^3 N_c / (8\pi^2)$ , and we have expressed the result in terms of the dimensionless variables defined in (3.14). We hence see that for our configuration, when there is non-vanishing value of chemical potential, the boundary Hamiltonian  $H_{\text{bdy}}$  is nonzero.

By adding to the action an extra surface term  $S_{\text{bdy}}$  which for our configuration takes the form

$$S_{\text{bdy}} = -2\kappa\tilde{\rho} \int d^4x dz \partial_z f, \quad (6.7)$$

one can remove the surface contribution to the equation of motion (3.3) which originates from the variation of the action (3.1). This addition also simultaneously cancels the boundary contribution to the Hamiltonian  $H_{\text{bdy}}$ . When comparing free energies of the various configurations in this paper, we therefore just need to compute the bulk contribution  $H_{\text{bulk}}$  to the Hamiltonian.

## 6.2 DBI-CS Hamiltonian

The DBI-CS Lagrangian can be written as

$$\mathcal{L} = -\frac{\gamma}{\sqrt{-g}}\sqrt{-E} + \frac{\alpha}{4\sqrt{-g}}\epsilon^{\ell mnpq}\mathcal{A}_\ell\mathcal{F}_{mn}\mathcal{F}_{pq}, \quad (6.8)$$

The conjugate momentum for the gauge field is given by

$$\Pi^a = \frac{\gamma\beta}{2\sqrt{-g}}\sqrt{-E}E^{(0,a)} + \frac{\alpha}{\sqrt{-g}}\epsilon^{0abcd}\mathcal{A}_b\mathcal{F}_{cd}, \quad (6.9)$$

so the corresponding Hamiltonian is

$$\begin{aligned} H_{\text{DBI-CS}} = & \int d^3\vec{x} dz \left\{ \gamma\sqrt{-E} \left[ 1 + \frac{\beta}{2}E^{(0,a)}\mathcal{F}_{0a} \right] + \partial_a \left[ \sqrt{-g}\Pi^a\mathcal{A}_0 \right] \right. \\ & \left. - \left[ \partial_a \left( \frac{\gamma\beta}{2}\sqrt{-E}E^{(0,a)} \right) + \frac{3}{4}\alpha\epsilon^{0abcd}\mathcal{F}_{ab}\mathcal{F}_{cd} \right] \mathcal{A}_0 \right\}. \end{aligned} \quad (6.10)$$

Note that the last term vanishes because it is just the 0th component of the DBI-CS equations.

Using the DBI-CS equations and the ansatz (3.10), the conjugate momentum reduces to

$$\Pi^i = 0 \quad , \quad \Pi^z = \frac{1}{\sqrt{-g}}(-\bar{\rho} + \alpha kh^2), \quad (6.11)$$

where  $\bar{\rho} = 2\kappa\tilde{\rho}$ . This is the same as the result (6.4) found for the Maxwell truncation. The boundary term in the action variation takes the form

$$\delta S_{\text{bdy}} = \bar{\rho} \int d^4x dz \partial_z \delta f, \quad (6.12)$$

so in order to obtain a stationary action we need to add the boundary term

$$\tilde{S} = -\bar{\rho} \int d^4x dz \partial_z f. \quad (6.13)$$

This term cancels the boundary term in the Hamiltonian. The bulk term takes the form

$$H_{\text{DBI-CS}} = 8\mathcal{H} \int dz K_z^{2/3} Q(z) \left[ 1 + \frac{1}{4}K_z^{1/3}(\partial_z \hat{h})^2 \right], \quad (6.14)$$

with  $Q(z)$  given by (4.11).

## References

- [1] D. V. Deryagin, D. Y. Grigoriev, and V. A. Rubakov, “Standing wave ground state in high density, zero temperature QCD at large- $N_c$ ”, *Int. J. Mod. Phys. A* **7** (1992) 659–681.
- [2] S. Nakamura, H. Ooguri, and C.-S. Park, “Gravity dual of spatially modulated phase”, *Phys. Rev. D* **81** (2010) 044018, [arXiv:0911.0679](#).
- [3] S. K. Domokos and J. A. Harvey, “Baryon number-induced Chern-Simons couplings of vector and axial-vector mesons in holographic QCD”, *Phys. Rev. Lett.* **99** (2007) 141602, [arXiv:0704.1604](#).
- [4] H. Ooguri and C.-S. Park, “Holographic end-point of spatially modulated phase transition”, *Phys. Rev. D* **82** (2010) 126001, [arXiv:1007.3737](#).
- [5] H. Ooguri and C.-S. Park, “Spatially modulated phase in holographic quark-gluon plasma”, *Phys. Rev. Lett.* **106** (2011) 061601, [arXiv:1011.4144](#).
- [6] T. Sakai and S. Sugimoto, “Low energy hadron physics in holographic QCD”, *Prog. Theor. Phys.* **113** (2005) 843–882, [hep-th/0412141](#).
- [7] T. Sakai and S. Sugimoto, “More on a holographic dual of QCD”, *Prog. Theor. Phys.* **114** (2006) 1083–1118, [hep-th/0507073](#).
- [8] O. Aharony, K. Peeters, J. Sonnenschein, and M. Zamaklar, “Rho meson condensation at finite isospin chemical potential in a holographic model for QCD”, *JHEP* **082** (2007) 1007, [arXiv:0709.3948](#).
- [9] K. Fukushima, D. E. Kharzeev, and H. J. Warringa, “The Chiral Magnetic Effect”, *Phys. Rev. D* **78** (2008) 074033, [arXiv:0808.3382](#).
- [10] K.-Y. Kim, B. Sahoo, and H.-U. Yee, “Holographic chiral magnetic spiral”, *JHEP* **10** (2010) 005, [arXiv:1007.1985](#).
- [11] W.-y. Chuang, S.-H. Dai, S. Kawamoto, F.-L. Lin, and C.-P. Yeh, “Dynamical instability of holographic QCD at finite density”, *Phys. Rev. D* **83** (2011) 106003, [arXiv:1004.0162](#).
- [12] M. N. Chernodub and A. S. Nedelin, “Phase diagram of chirally imbalanced QCD matter”, [arXiv:1102.0188](#).
- [13] H. W. Braden, J. D. Brown, B. F. Whiting, and J. W. York, Jr., “Charged black hole in a grand canonical ensemble”, *Phys. Rev. D* **42** (1990) 3376–3385.
- [14] M. Ruggieri, “The critical end point of Quantum Chromodynamics detected by chirally imbalanced quark matter”, [arXiv:1103.6186](#).